RESEARCH ARTICLE

INTERNATIONAL RESEARCH JOURNAL OF MULTIDISCIPLINARY TECHNOVATION

Asian Research Association

DOI: 10.54392/irjmt2446

A Versatile Electrochemical Sensor Polyaniline–Polypyrrole Co-Polymer for the Ultra-Sensitive Quercetin Detection

P. Jency Sebatine [a], S. Muthamizh [b,*], R. Mohan Kumar [a]

[a] Department of Physics, Presidency College, Chennai-600005, Tamil Nadu, India

[b] Department of Physiology, Saveetha Dental College and Hospitals, Saveetha Institute of Medical and Technical Sciences, Saveetha University, Chennai-600077, Tamil Nadu, India

* Corresponding Author Email: muthamizh23@ymail.com

DOI: https://doi.org/10.54392/irjmt2446

Received: 10-05-2024; Revised: 11-07-2024; Accepted: 17-07-2024; Published: 30-07-2024

Abstract: Quercetin has been shown to enhance inflammation, blood pressure, and blood sugar control. It may also have brain-protective, anti-allergy, and anticancer effects. In this work, a chemical oxidative polymerization approach is employed to synthesis of PANI-PPy copolymer for electrochemical biosensing of quercetin molecule. Unique, sustainable, low-cost, and simple to use, a synthesis of PANI-pPY copolymer has been achieved. The prepared PANI-PPy copolymer characterized with different technique like XRD, FT-IR, Raman, XPS, FESEM with EDAX and HR-TEM for identifying crystalline nature, functional group band gap, chemical composition, and morphology respectively. The surface morphology of the synthesized copolymers were in homogenous sphere like architecture. Synthesized copolymer is modified on glassy carbon electrode (GCE) to senses the biomolecule (Quercetin) by electrochemical method. PANI-PPy copolymer will greatly enhance the electrocatalytic oxidation of Quercetin (QR). The detection limit and quantification limit have been worked out to be 11.2 and 37.34 µM μA^{-1}, respectively at neutral pH. All of the findings suggest that the PANI-PPy modified GCE is more sensitive to the oxidation of Quercetin. Eventually, the synthesized PANI-PPy hybrid may be used in catalysis research in addition to analytical laboratories due to its advantageous properties of enhanced catalytic activity and electrochemical sensitivity.

Keywords: PANI-PPy, Conducting Polymers, Electrochemical Sensing, Flavonoid.

1. Introduction

Electronic conducting polymers have been extensively explored. Among the class of conducting polymers, polyaniline (PANI) and polypyrrole (PPy) stand out as highly desirable materials due to their excellent electrical conductivity [1]. These polymers are environmentally resilient due to their ability to recover from environmental stresses or disruptions without suffering severe, long-term harm or degradation. (PANI) and polypyrrole (PPy) have advantageous physiochemical characteristics and cost-effectiveness in production [2]. These characteristics create advantageous circumstances for potential use in a different of applications, including solar cells, diodes, electrochemical sensors and supercapacitor.[3-6] PANI and PPy can be produced via chemical oxidative polymerization, electrochemical methods, and they can be altered to switch between their conductive and non-conductive states [7]. Phytonutrients, or plant chemicals, include flavonoids. The most prevalent flavonoid is quercetin. It belongs to the flavonoids family and is a type of precursor to polyphenols. It is prevalent in all natural plant tissues, including leaves, stems, and roots. The majority of fruits and vegetables contain this active ingredient [8]. Quercetin contains an assortment of flavonoid glycosides in the form of aglycone. Through interaction, this quercetin greatly adds to the biotic characteristics. It is thought that quercetin, an antioxidant, benefits the human body in the right amounts and may lower blood pressure and fat levels. As a result, it is frequently used to treat neurological and coronary problems. Quercetin is also employed in the enhancement of respiratory immunity because of its special immune-stimulating effects. It suppresses inflammation and regulates the immune system in many forms of autoimmune disease [9]. Additionally, it promotes and maintains intestinal lining cells, allowing for the treatment of gastric and duodenal ulcers as well as inflammatory bowel disease. The study of quercetin has been carried out using a variety of approaches, including spectrophotometry, gas chromatography with mass spectrometry, high-performance liquid chromatography, colorimetric methods, and electrochemical procedures. When it comes to meeting the demands of scientific and industrial research, electrochemical methods are among the most important [10]. While some of these technologies allow for the

quantification of quercetin using a variety of fundamental concepts, the others all have low sensitivity and difficult modification. Electrochemistry-based methods have an edge over other methods. Since electrochemical sensors only require a little volume or quantity of the sample for the electrochemical analysis, they are useful and effective for the detection and monitoring of contaminants in environmental samples. Greater sensitivity, quicker kinetics, less solvent use, and environmental friendliness are benefits of the electrochemical method. But due to appealing advantages including high sensitivity, quick response time, cost effectiveness, and low detection limit, electrochemical sensing technology is more promising for detecting quercetin [11].

The present investigation proceeds with the synthesis of PANI-PPy nanocomposites by oxidative polymerization method and tested for electrochemical sensing of the flavonoid quercetin. The formation of polymer composites was confirmed by various characterization techniques like XRD, FTIR, Raman, morphological analysis was done by utilizing FE-SEM, HR-TEM and chemical composition was investigated by XPS analysis respectively. Using cyclic voltammetry (CV), quercetin was determined electrochemically and differential pulls voltammetry (DPV).

2. Experimental

2.1. Materials and Methods

Aniline, pyrrole, Ammonium persulphate, p-hydroxyl benzene sulphonic acid, were purchased from Qualigens. Quercetin from Sigma Aldrich were used as received. Distilled aniline, pyrrole and double distilled water, ethanol were used throughout the experiment.

2.2. Fabrication of PANI-Ppy by Oxidative Chemical Polymerization Method

In synthesis process, a mixture of binary monomers aniline and pyrrole with different ratio like 25;75, 50;50 and 75;25 and p-hydroxyl benzene sulphonic acid (10 mM) were taken in a three neck round bottom flask, to the above solution 180 mL of DD water was added. The reaction medium was maintained at ice cooled condition under constant magnetic stirring condition. Then, 14 nM concentration of aqueous ammonium persulfate solution (25 mL) was taken in burette allowed drop wise addition to the above reaction solution under stirring condition. After the addition process complete the solution was subjected to stirring for 24 h. Final product was found to appear like green-black in colour which was collected by centrifugation procedure. The sample was splashed with mixed solvent of ethanol and DD water. The product was dried under vacuum and kept in a desiccator. In the present work we have synthesized the PANI-PPy conducting co-polymer according to ration named as S1, S2 and S3.

3. Results and Discussion

3.1 XRD analysis

The XRD pattern of PANI-PPy co-polymer S1, S2 and S3 are shown in Figure.1. In all the three samples a broad peak centered at 23.73° is detected for copolymer Nano spheres, reason for the peak is intermolecular interaction between pyrrole units and PANI units. A broad peak indicates the presence of amorphous nature of the copolymer [12].

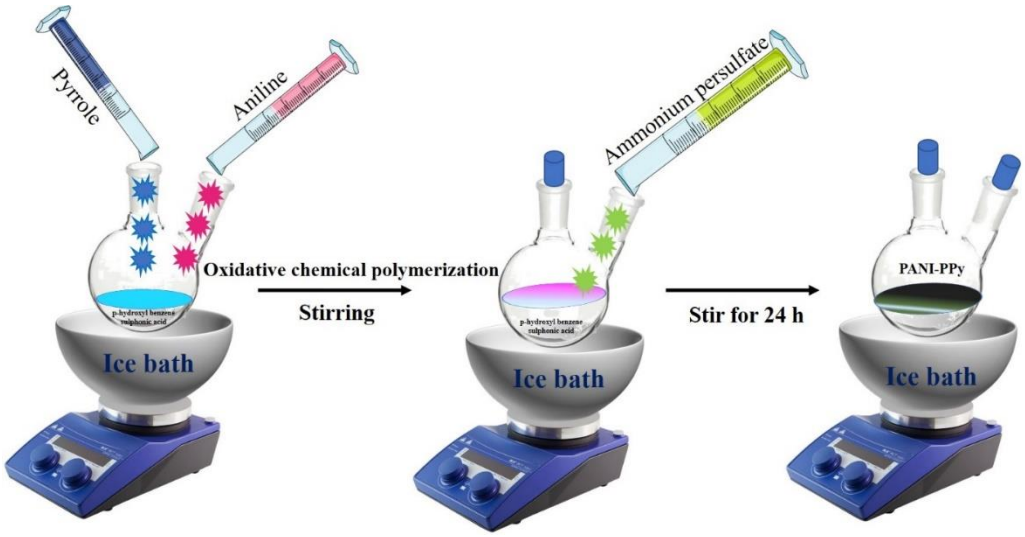

Scheme 1. Synthesis of PANI-PPy by Oxidative chemical polymerization method.

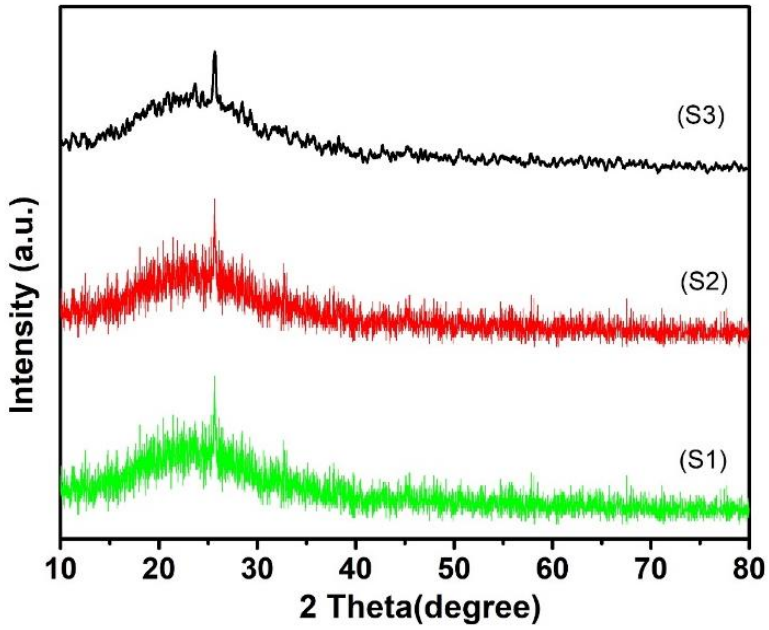

Figure 1. XRD pattern of PANI-PPy S1 (25; 75), S2 (50; 50) and S3 (75; 25) respectively

3.2 Raman Analysis

The Raman spectra of S1, S2 and S3 copolymer sample are given in Figure 2. The Raman spectrum of PANI-PPy displays the peaks at 1168, 1247, 1336, 1469, and 1594 cm^{-1}. The Raman peak at 1168 cm^{-1} is owing to the presence of in-plane bending of C-H group in benzenoid ring of polymeric unit. Peak located at 1247 cm^{-1} is owing to the occurrence of bipolaron structure present in the compound which represents the emeraldine state [13]. The peak at 1336 cm^{-1} is related with the polaron through doping procedure [14]. Furthermore, the peak perceived at 1469 and 1594 cm^{-1} are naturally accredited to the quinoid rings C=N and C=C stretching vibrations, respectively, which are derived from bipolaron structures [15].

3.3 FTIR Analysis

The FTIR spectra of different ratio of PANI-PPy nanospheres named as S1, S2 and S3 are shown in Figure 3. Bands at 2989 and 2346 cm^{-1} belong to the characteristic of N-H bond of aromatic amines present in the compound [16]. Because of the protonated quinoid and benzenoid rings stretching modes, PANI-PPy displays bands at 1559 and 1485 cm^{-1} that provide the term of the PANI-PPy backbone [12]. The secondary aromatic amine's C-N stretching manner is responsible for the peak at 1214 [17]. C-H in-plane bending in the aromatic structure is indicated by two bands at 1168 and 1120 cm^{-1} [18]. Moreover, the symmetric S-O stretch is allocated to the band at 1049 cm^{-1}, while the asymmetric S-O stretch is assigned to the band at 928 cm^{-1}. The existence of C-H bending mode and C-H plane deformation vibration is responsible for the bands at 754 and 689 cm^{-1} [19]. Thus, it was shown by the FTIR spectrum data that PANI-PPy were produced and existed in the conducting emeraldine form [20].

3.4 XPS Analysis

The XPS survey spectrum of PANI-PPy (50:50) S2 nanospheres is displayed in Figure 4 (a-e). Figure. 4 (a) displays the survey spectrum of S2 which represents shows the presence of C, N and O. Figure. 4 (b) displays the core level spectrum of C 1s with three split peaks, the peak associated to binding energy at 284.36 eV is confirms C–C group that presence in the aromatic ring of polymeric unit. The second peak, 285.52 eV is due to the C–N bonds. The feature at 288.84 eV can be attributed to C-N [21, 22]. Figure. 4 (c) displays the XPS core level spectrum of the N 1S in the S2. Broad peaks centered at about 399.95 eV which is corresponding to -NH- polymer group [23]. Figure. 4 (d) displays the XPS core level spectra of the O 1S. The peak is centered at about 529.30 eV and 530.52 eV and is very broad, since the source of this signal will be the polymer lattice [24]. Figure. 4 (e) displays the XPS spectra of the S 1S core level in the PANI-PPy. The two peak is centered at about 164.25, 165.48 eV and is very broad [25].

3.5 Morphological Examination

The FE-SEM image of synthesized PANI-PPy (S2) was done. Visualized images confirms that spheres like morphology of the fabricated PANI-PPy which are represented in Figure. 5(a-d) with magnification varies from 500-200 nm**.** The shape and crystallinity of PANI-PPy were further confirmed by HR-TEM investigation. As observed in FE-SEM, HR-TEM also confirms the spherical morphology of the polymer composite. EDAX analysis was done for the same sample for the identification of the elements presents, graph shows that

presence of C, N, and O as expected. In Figure. 6(c), the HR-TEM morphology of PANI-PPy nanospheres is shown. Amorphous PANI-PPy nanospheres are clearly shown by the SAED pattern of the produced polymer composite shown in Figure. 5(d), which is in good agreement with the XRD results [26].

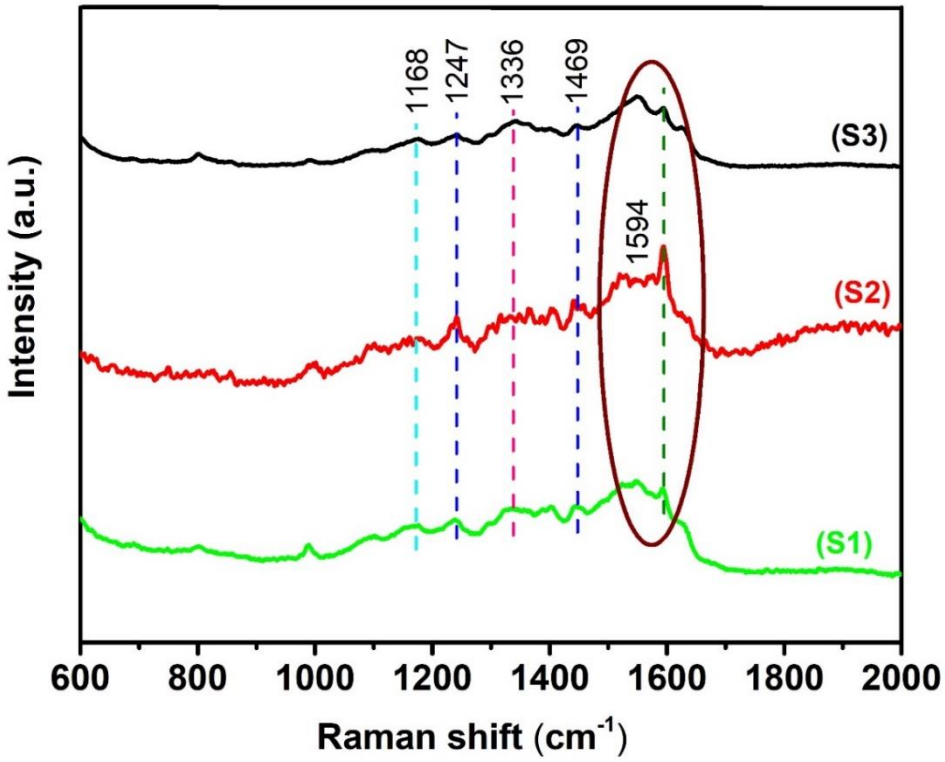

Figure 2. Raman spectrum of PANI-PPy S1 (25; 75), S2 (50; 50) and S3 (75; 25) respectively

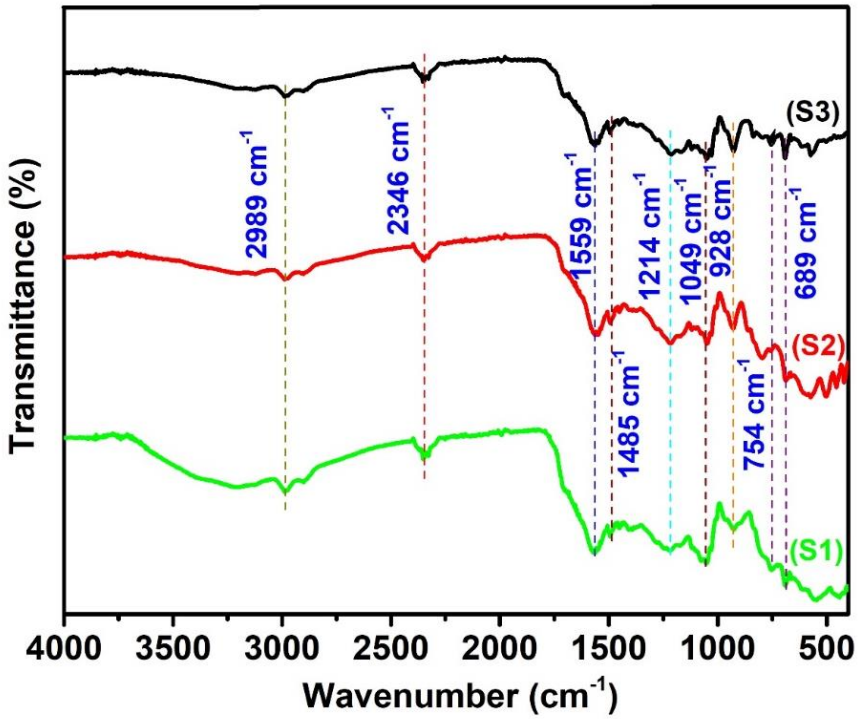

Figure 3. FT-IR spectrum of PANI-PPy S1 (25; 75), S2 (50; 50) and S3 (75;25) respectively

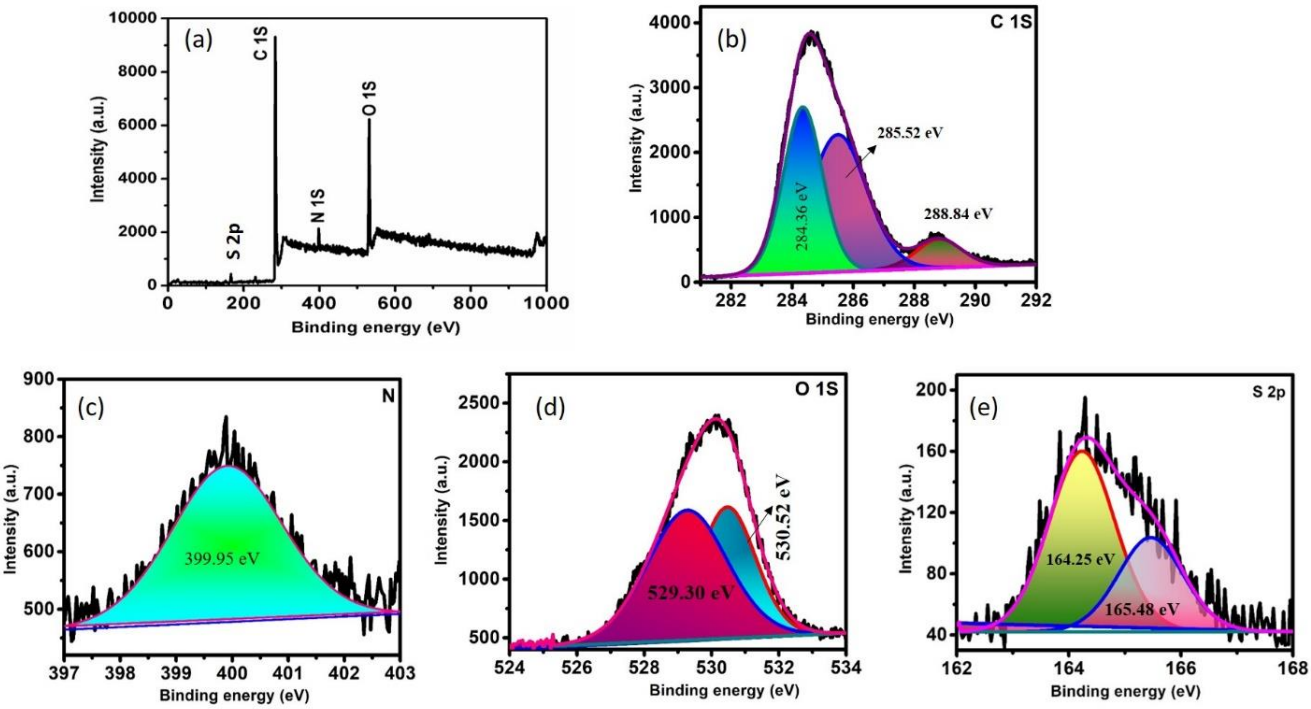

Figure 4. (a) XPS Survey spectrum; (b) XPS core level spectrum of S; (c) XPS core level spectrum of O; (d) XPS core level spectrum of N; and (e) XPS core level spectrum of C of S2 PANI-PPy (50;50).

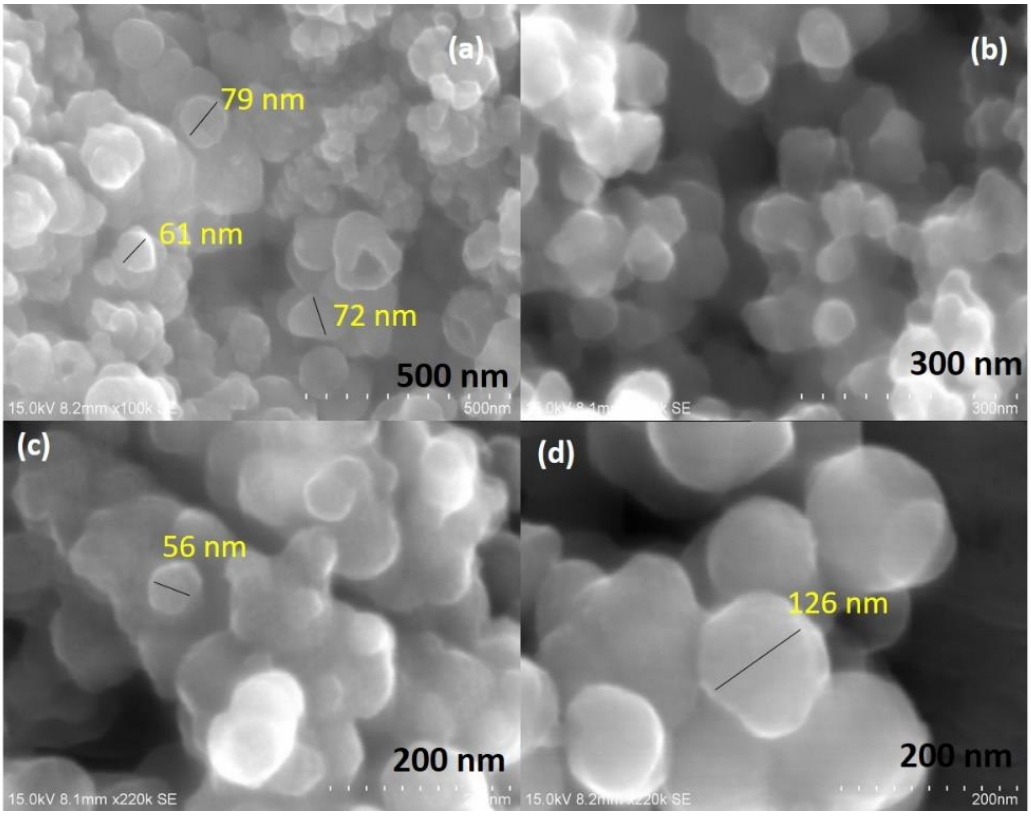

Figure 5. (a-d) FE-SEM images of synthesized PANI-PPy nanosphers

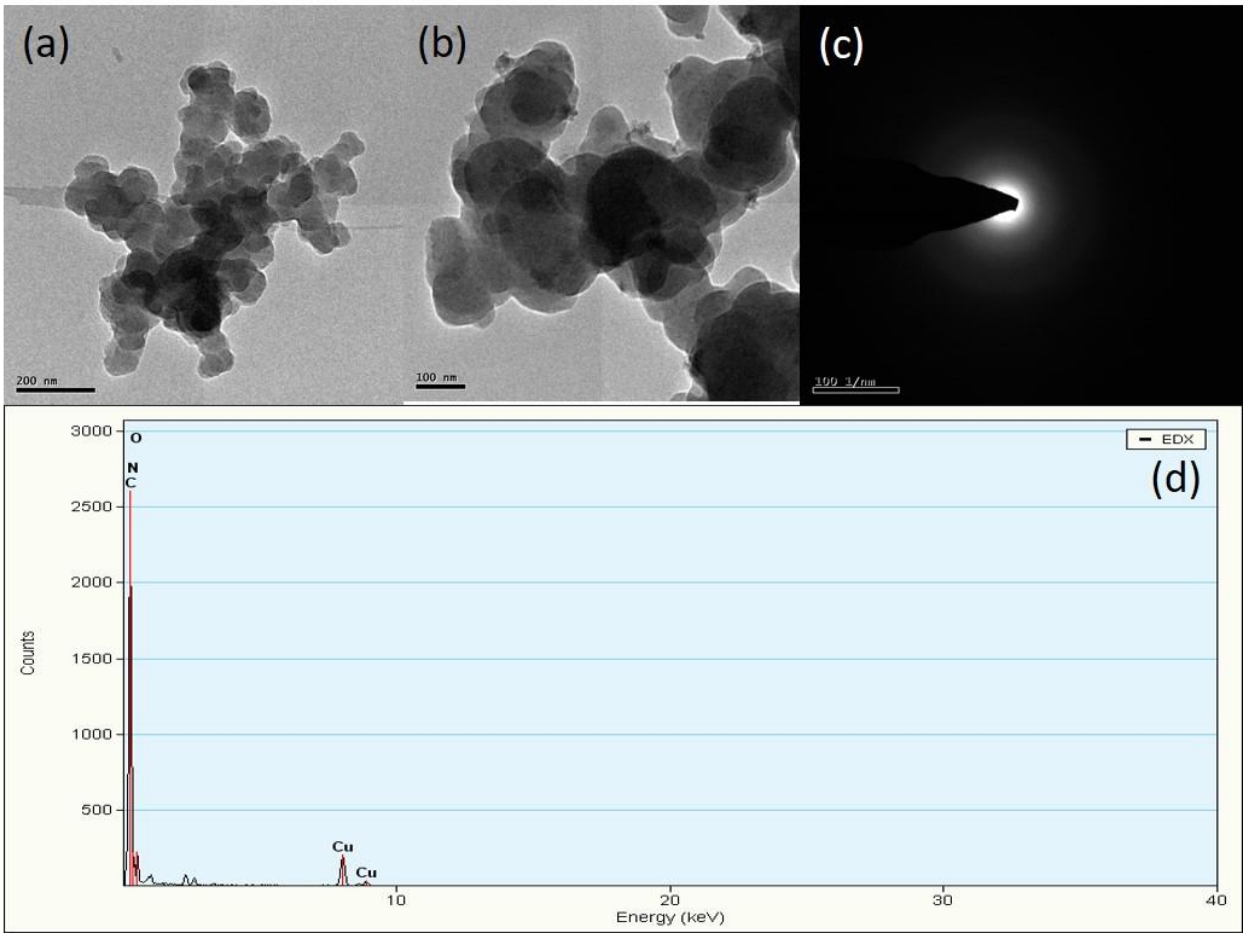

Figure 6. (a-b) HR-TEM images, (c) SAED pattern and (d) EDX of synthesized PANI-PPy Nano spheres respectively.

4. Electrochemical sensing of quercetin

4.1. Cyclic voltammetry of QA at PANI-PPy /GCE

Synthesized PANI-PPy was utilized for the modification of working electrode for sensing the biomolecule quercetin. The cyclic voltammetric responses of the unmodified GCE and PANI-PPy modified GCE to quercetin were investigated at neutral pH 7 at a scan rate of 50 mVs-1, as shown in Figure. 7. Anodic peak current was noted to be 2.52 µA for the bare GCE electrode for quercetin sensing and PANI-PPy modified GCE sense the quercetin with higher current response than bare GCE as 5.3 µA. When compare to bare GCE the modified GCE shows the higher current response which indicates the higher sensing ability of the synthesized catalyst [27]. The existence of a greater surface area and homogenous shape may be the primary cause of the improved electrochemical activity. Therefore, quercetin may be detected at lower potential with improved current responsiveness using the S2 sample modified GCE.

4.2. The influence of pH on Quercetin electrochemical sensing

With a pH solution ranging from 3 to 11, the impact of pH on the electrochemical oxidation of quercetin at a concentration of 0.1 mM at PANI-PPy/GCE was observed using the cyclic voltammetry technique. Observed outcomes are exhibited in the Figure. 8**.** From the figure we have noticed that as the pH of the medium upsurges the cyclic voltammograms become wider with difference in peak current. At lower pH of 3 the anodic peak potential was measured at 0.41 V, when rise in the pH of the medium up to 11 the peak potential noted to be -0.0046 V. Comparing the peak current and peak potential of obtained results indicates that there is uniform decrease in the current and potential up to pH 6. The current response is 5.03 µA greater at neutral pH 7. Beyond pH 7, peak potential and peak current both decrease dramatically. The pH of the reaction was tuned to be seven based on the aforementioned finding. The anodic peak potential (E_{pa}) of quercetin decreases linearly (Figure 8 inset) with a linear regression equation E_{pa} (V) = -0.0632 pH + 0.63032 (R^2 =0.9716) close to that given by the According to the Nernst equation, quercetin undergoes electro-oxidation on the electrode surface when an equal amount of protons and electrons are present. Using the Nernst equation, Epa = E - [(2.303mRT)/(nF)] pH, the ratio of m/n was found to be 2, where n is the number of electrons transported, m is the number of protons intervening in the oxidation process, and R, T, and F have the standard definitions [28].

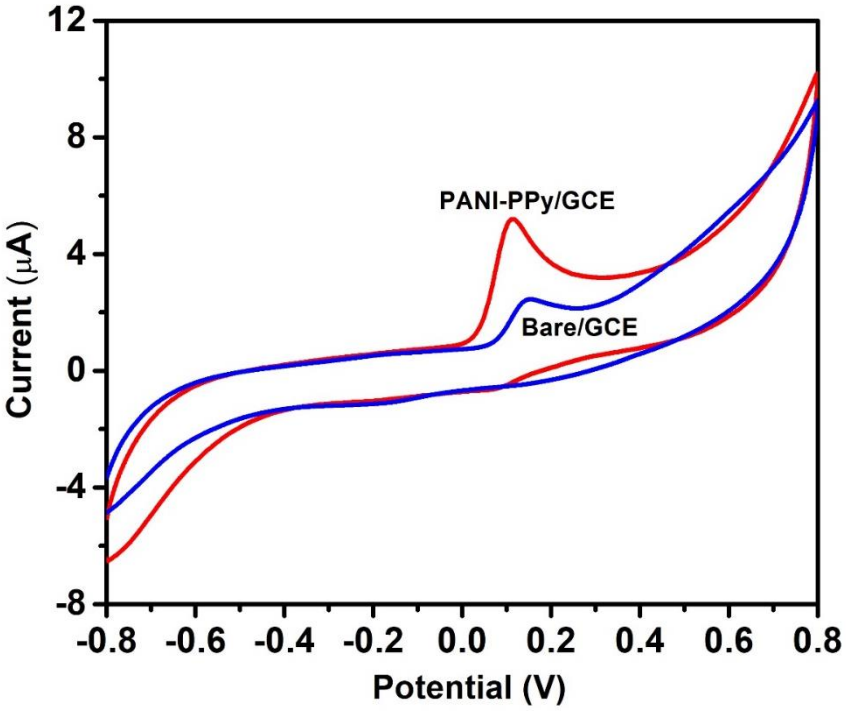

Figure 7. Cyclic voltammograms of (a) bare GCE and (b) PANI-PPy/GCE in pH 7 at the scan rate of 50 mVs^{-1}.

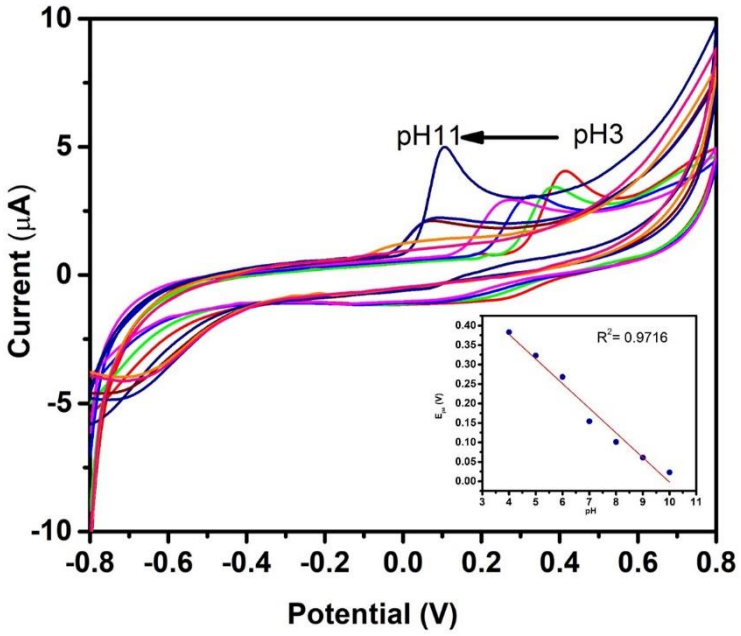

Figure 8. PANI-PPy/GCE cyclic voltammograms at various pH values observed at a scan rate of 50 mVs-1. Anodic potential vs. pH is shown linearly in the insert.

With knowledge of the electron transfer number, the proton transfer number may be computed.

4.3. Scan Rate Effect on the Electrochemical Performance

An investigation was conducted on the impact of scan rate on the electro oxidation of 0.1 mM quercetin obtained results displayed in Figure 9 (a). The electrode kinetics for quercetin oxidation were studied by examining the dependence of quercetin electro oxidation with varying scan speeds. We could see that the peak current of quercetin rose together with the scan rate. Plotting a double logarithmic plot revealed the electrode response, whether it was a surface limited process or diffusion process. As can be seen from Figure 9 (b), the electrode response is a adsorption-controlled process, as evidenced by the slope value of 1.48 [29].

4.4. The total number of protons and electrons transferred during the electrochemical oxidation process of quercetin

Quercetin is oxidized at the PANI-PPy modified GCE electrode by the transfer of electrons and protons. The following equation used to determine how many electrons are interchanged when quercetin is electrochemically oxidized at the GCE.

$$i_p = nFQu/4RT$$

Where n, i_p, R, T, F, Q, υ have their usual meanings. By inserting the constant values in the above equation number of electron (n) intricate in the oxidation of quercetin is 2. The ratio of m/n = 1. As a result, it was determined that the proton transfer number was 2. This leads us to the conclusion that quercetin electro oxidation at the PANI-PPy/GCE comprises a two electron and two proton progression [30]. The quantity of protons and electrons determined for the oxidation of quercetin amply demonstrates that quinone is formed by the method shown in Scheme 2**.**

4.5. Differential pulse voltammetry of QA at PANI-PPy/GCE

In order to prepare a calibration curve for the QA analysis, differential pulse voltammetry (DPV), which has comparatively superior current sensitivity and resolution than cyclic voltammetry, is used. Fig.10. Represents the DPV response of QA oxidation at PANI-PPy/GCE in pH7. It is evident that across the concentration range of QA, the oxidation peak current progressively increases from 1.99 × 10^{-6} to 25.34 ×10^{-6} M. The graph used to calibrate the QA determination by the PANI-PPy/GCE is presented as an insert in Fig.10. The linear regression equation is found as I_a(μA) = 0.01 [QA] (μM) + 1.145 (R^2 = 0.9873) with a sensitivity of 1.053 μA/μM, shows that the PANI-PPy/GCE is highly sensitive towards QA. The detection limit (DL) and quantification limit (QL) were calculated from Eq-1 and Eq-2 respectively.

$$DL = 3s/b \quad (1)$$

$$QL = 10s/b \quad (2)$$

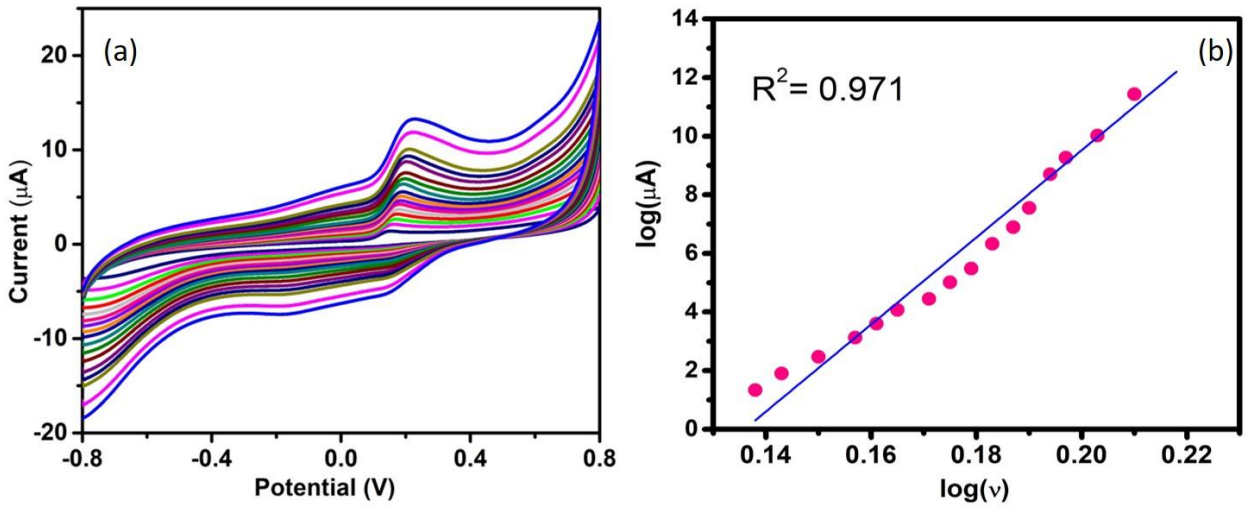

Figure 9. Cyclic voltammograms of PANI-PPy/GCE in pH 7 at the scan rate from 10-500 mVs-1. Inset shows the log (ipa) vs log (υ) plot.

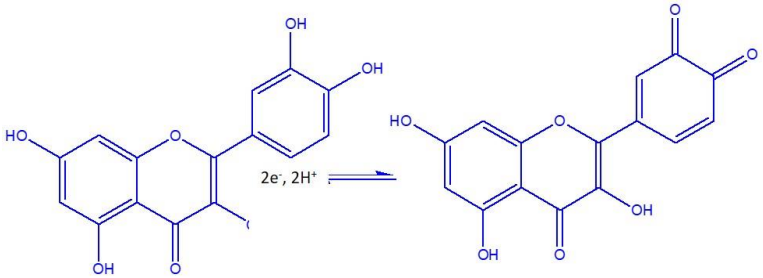

Scheme 2. Electro oxidation mechanism of quercetin

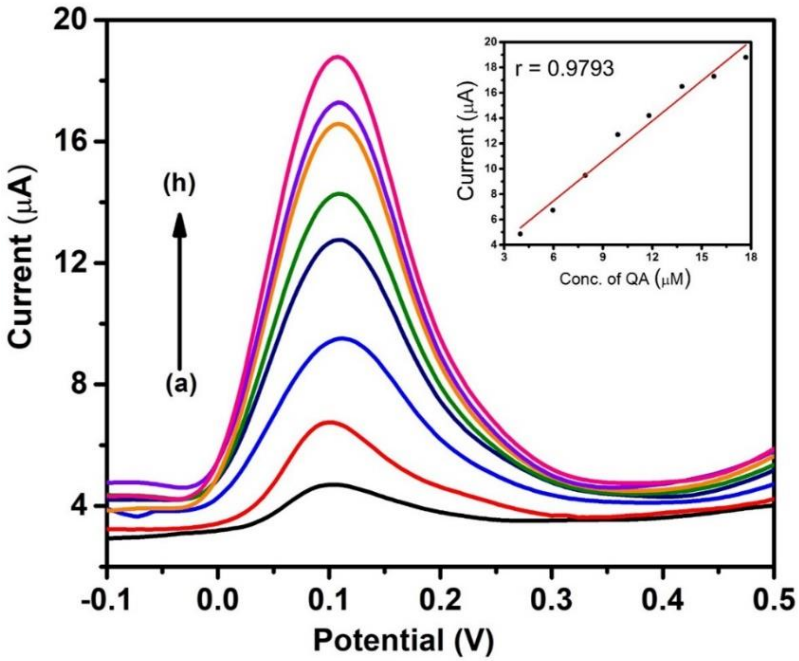

Figure 10. Differential pulse voltammetric responses of PANI-PPy/GCE in pH 6 containing various [QA] from (a) to (h): 1.9, 3.9, 5.9, 7.9, 9.9, 11.8, 13.8, and 15.74 μM. Scan rate: 50 mVs-1. Inset is the plot of current versus concentration of QA

Where s represents the standard deviation and b is the slope of the calibration curve. The calculated DL and QL are 11.2 μM μA^{-1} and 37.34 μM μA^{-1} respectively. The whole observations suggest that the PANI-PPy/GCE has a comparatively increased sensitivity to oxidation of QA depends on the concentration.

5. Conclusion

In summary, PANI-PPy with three distinct ratios was effectively synthesized in this study by using a simple oxidative chemical polymerization process, and it was subsequently utilized to build an electrochemical sensor for the sensitive and targeted detection of QR. The huge surface area of PANI-PPy for quercetin adsorption and strong conductivity for quick electron transport were the reasons for the remarkable performance of the suggested working electrode. The obtained results further demonstrate the strong sensitivity of 1.053 μA/μM and excellent limit of detection (LOD) and limit of quantification of 11.2 μM/μA and 37.34 μM/μA of the proposed electrochemical sensor. One potential sensor material for Quercetin detection was the synthesized PANI-PPy.

References

[1] M.M.R. Khan, M. Islam, M.K. Amin, S.K. Paul, S. Rahman, M.M. Talukder, M.M. Rahman, Simplistic fabrication of aniline and pyrrole-based poly (Ani-co-Py) for efficient photocatalytic performance and supercapacitors. International Journal of Hydrogen Energy, 47(89), (2022) 37860-37869. https://doi.org/10.1016/j.ijhydene.2022.08.296

[2] J. Stejskal, Recent advances in the removal of organic dyes from aqueous media with conducting polymers, polyaniline and polypyrrole, and their composites. Polymers, 14(19), (2022) 4243. https://doi.org/10.3390/polym14194243

[3] P. Pattanayak, F. Papiya, V. Kumar, A. Singh, P.P. Kundu, Performance evaluation of poly (aniline-co-pyrrole) wrapped titanium dioxide nanocomposite as an air-cathode catalyst material for microbial fuel cell. Materials Science and Engineering: C, 118, (2021) 111492. https://doi.org/10.1016/j.msec.2020.111492

[4] S. Dhibar, P. Bhattacharya, G. Hatui, C.K. Das, Transition metal doped poly (aniline-co-pyrrole)/multi-walled carbon nanotubes nanocomposite for high performance supercapacitor electrode materials. Journal of Alloys and Compounds, 625, (2015) 64-75. https://doi.org/10.1016/j.jallcom.2014.11.108

[5] A. Moyseowicz, Z. González, R. Menéndez, G. Gryglewicz, Three-dimensional poly (aniline-co-pyrrole)/thermally reduced graphene oxide composite as a binder-free electrode for high-performance supercapacitors. Composites Part B: Engineering, 145, (2018) 232-239. https://doi.org/10.1016/j.compositesb.2018.03.018

[6] D. Lv, W. Shen, W. Chen, Y. Wang, R. Tan, M. Zhao, W. Song, Emerging poly (aniline co-pyrrole) nanocomposites by in-situ polymerized for high-performance flexible ammonia sensor. Sensors and Actuators A: Physical, 349, (2023)

114078. https://doi.org/10.1016/j.sna.2022.114078

[7] N.Y. Abu-Thabit, Chemical oxidative polymerization of polyaniline: A practical approach for preparation of smart conductive textiles. Journal of Chemical Education, 93(9), (2016)1606-1611. https://doi.org/10.1021/acs.jchemed.6b00060

[8] L. Liv, E. Karakus, Signal-enhanced electrochemical determination of quercetin with poly (Chromotrope Fb)-modified pencil graphite electrode in vegetables and fruits. ACS omega, 8(13), (2023) 12522-12531. https://doi.org/10.1021/acsomega.3c00599

[9] V. Mariyappan, N. Karuppusamy, S.M. Chen, P. Raja, R. Ramachandran, Electrochemical determination of quercetin using glassy carbon electrode modified with WS2/GdCoO3 nanocomposite. Microchimica Acta, 189(3), (2022) 118. https://doi.org/10.1007/s00604-022-05219-3

[10] S. Muthamizh, R. Suresh, K. Giribabu, R. Manigandan, S.P. Kumar, S. Munusamy, V. Narayanan, MnWO4 nanocapsules: synthesis, characterization and its electrochemical sensing property. Journal of Alloys and Compounds, 619, (2015) 601-609. https://doi.org/10.1016/j.jallcom.2014.09.049

[11] Z. Yao, X. Yang, X. Liu, Y. Yang, Y. Hu, Z. Zhao, Electrochemical quercetin sensor based on a nanocomposite consisting of magnetized reduced graphene oxide, silver nanoparticles and a molecularly imprinted polymer on a screen-printed electrode. Microchimica Acta, 185, (2018) 1-9. https://doi.org/10.1007/s00604-017-2613-5

[12] V.D. Thao, B.L. Giang, T.V. Thu, Free-standing polypyrrole/polyaniline composite film fabricated by interfacial polymerization at the vapor/liquid interface for enhanced hexavalent chromium adsorption. RSC advances, 9(10), (2019) 5445-5452. https://doi.org/10.1039/C8RA10478F

[13] G. Liao, Green preparation of sulfonated polystyrene/polyaniline/silver composites with enhanced anticorrosive properties. International Journal of Chemistry, 10(1), (2018) 81-86. https://doi.org/10.5539/ijc.v10n1p81

[14] R. Kandulna, R.B. Choudhary, R. Singh, Free exciton absorptions and quasi-reversible redox actions in polypyrrole–polyaniline–zinc oxide nanocomposites as electron transporting layer for organic light emitting diode and electrode material for supercapacitors. Journal of Inorganic and Organometallic Polymers and Materials, 29, (2019) 730-744. https://doi.org/10.1007/s10904-018-1047-9

[15] M.Y. Abed, M.A. Youssif, H.A. Aziz, M.A. Shenashen, Synthesis and enhancing electrical properties of PAni and PPA composites. Egyptian Journal of Petroleum, 23(3), (2014) 271-277. https://doi.org/10.1016/j.ejpe.2014.08.003

[16] Y. Wang, J. Yang, L. Wang, K. Du, Q. Yin, Q. Yin, Polypyrrole/graphene/polyaniline ternary nanocomposite with high thermoelectric power factor. ACS applied materials & interfaces, 9(23), (2017) 20124-20131. https://doi.org/10.1021/acsami.7b05357

[17] M. Trchová, J. Stejskal, Resonance Raman spectroscopy of conducting polypyrrole nanotubes: disordered surface versus ordered body. The Journal of Physical Chemistry A, 122(48), (2018) 9298-9306. https://doi.org/10.1021/acs.jpca.8b09794

[18] W. Lu, S. Yin, X. Wu, Q. Luo, E. Wang, L. Cui, C.Y. Guo, Aniline–pyrrole copolymers formed on single-walled carbon nanotubes with enhanced thermoelectric performance. Journal of Materials Chemistry C, 9(8), (2021) 2898-2903. https://doi.org/10.1039/D0TC05757F

[19] W. Zhao, Y. Wang, A. Wang, Nonlinear optical properties of novel polypyrrole derivatives bearing different aromatic segments. Materials Sciences and Applications, 8(11), (2017) 774-783. https://doi.org/10.4236/msa.2017.811056

[20] V.T. Santana, O.R. Nascimento, D. Djurado, J.P. Travers, A. Pron, L. Walmsley, Evidence of weak ferromagnetism in doped plasticized polyaniline (PANI–DDoESSA) 0.5 from electron spin resonance measurements. Journal of Physics: Condensed Matter, 25(11), (2013) 116004. https://doi.org/10.1088/0953-8984/25/11/116004

[21] P. Ahuja, S.K. Ujjain, I. Arora, M. Samim, Hierarchically grown NiO-decorated polyaniline-reduced graphene oxide composite for ultrafast sunlight-driven photocatalysis. ACS omega, 3(7), (2018) 7846-7855. https://doi.org/10.1021/acsomega.8b00765

[22] F. Liu, S. Luo, D. Liu, W. Chen, , Huang, Y., Dong, L., & Wang, L. (2017). Facile processing of free-standing polyaniline/SWCNT film as an integrated electrode for flexible supercapacitor application. ACS applied materials & interfaces, 9(39), 33791-33801. https://doi.org/10.1021/acsami.7b08382

[23] H. Peng, G. Ma, K. Sun, J. Mu, X. Zhou, Z. Lei, A novel fabrication of nitrogen-containing carbon nanospheres with high rate capability as electrode materials for supercapacitors. Rsc Advances, 5(16), (2015) 12034-12042. https://doi.org/10.1039/C4RA11889H

[24] M. Setka, R. Calavia, L. Vojkuvka, E. Llobet, J. Drbohlavová, S. Vallejos, Raman and XPS studies of ammonia sensitive polypyrrole nanorods and nanoparticles. Scientific reports, 9(1), (2019) 8465. https://doi.org/10.1038/s41598-019-44900-1

[25] F.P. Du, N.N. Cao, Y.F. Zhang, P. Fu, Y.G. Wu, Z.D. Lin, R. Shi, A. Amini, C. Cheng, PEDOT:

PSS/graphene quantum dots films with enhanced thermoelectric properties via strong interfacial interaction and phase separation. Scientific Reports, 8(1), (2018) 6441. https://doi.org/10.1038/s41598-018-24632-4

[26] Y. Wang, W.B. Ma, L. Guo, X.Z. Song, X.Y. Tao, L.T. Guo,. H.L. Fan, Z.S. Liu, Y.B. Zhu, X.Y. Wei, Phytic acid-doped poly (aniline-co-pyrrole) copolymers for supercapacitor electrodes applications. Journal of Materials Science: Materials in Electronics, 31, (2020) 6263-6273. https://doi.org/10.1007/s10854-020-03181-5

[27] T. Tang, M. Zhou, J. Lv, H. Cheng, H. Wang, D. Qin, G. Qin, G.Hu, X. Liu, Sensitive and selective electrochemical determination of uric acid in urine based on ultrasmall iron oxide nanoparticles decorated urchin-like nitrogen-doped carbon. Colloids and Surfaces B: Biointerfaces, 216, (2022) 112538. https://doi.org/10.1016/j.colsurfb.2022.112538

[28] Z. Zhou, P. Zhao, C. Wang, P. Yang, Y. Xie, J. Fei, Ultra-sensitive amperometric determination of quercetin by using a glassy carbon electrode modified with a nanocomposite prepared from aminated graphene quantum dots, thiolated β-cyclodextrin and gold nanoparticles. Microchimica Acta, 187, (2020) 1-9. https://doi.org/10.1007/s00604-019-4106-1

[29] V.V. Tkach, J.I.F. da Paiva Martins, Z.M. Romanova, V.V. Paientko, S.C. de Oliveira, J.R. Garcia, O.V. Skrypska, Y.G. Ivanushko, P.I. Yagodynets, The Theoretical Description for Aesculetin and Quercetin Cathodic Electrochemical Determination in Wines. In Medical Sciences Forum, 23(1), (2023) 4. https://doi.org/10.3390/msf2023023004

[30] F. Gao, W. Hong, B. Xu, Y. Wang, L. Lu, Z. Zhao, C. Zhang, X. Deng, J. Tang, Mxene nanosheets decorated with Pt nanostructures for the selective electrochemical detection of quercetin. ACS Applied Nano Materials, 6(8), (2023) 6869-6878. https://doi.org/10.1021/acsanm.3c00584

Authors Contribution Statement

P. Jency Sebatine- Conceptualization, methodology, software formal analysis, writing—original draft preparation, writing—review and editing. **S. Muthamizh**- Conceptualization, methodology, investigation, writing—original draft preparation, writing—review and editing, supervision. **R. Mohan Kumar**- Conceptualization, methodology, investigation, writing—original draft preparation, writing—review and editing. All the authors read and approved the final version of the manuscript.

Funding

The authors declare that no funds, grants or any other support were received during the preparation of this manuscript.

Competing Interests

The authors declare that there are no conflicts of interest regarding the publication of this manuscript.

Data Availability

The data supporting the findings of this study can be obtained from the corresponding author upon reasonable request.

Has this article screened for similarity?

Yes

About the License